Identification of the Active Conformation and the Importance of Length of the Flexible Loop 72−83 in Regulating the Conformational Change of Undecaprenyl Pyrophosphate Synthase†

Sing-Yang Chang, Yi-Kai Chen, Andrew H.-J. Wang,* and Po-Huang Liang*

Institute of Biological Chemistry, Academia Sinica, Taipei 11529, Taiwan

Received July 20, 2003; Revised Manuscript Received October 1, 2003

ABSTRACT: Increasing evidence has shown that intrinsic disorder of proteins plays a key role in their biological functions. In the case of undecaprenyl pyrophosphate synthase (UPPs), which catalyzes the chain elongation of farnesyl pyrophosphate (FPP) to undecaprenyl pyrophosphate via eight consecutive condensation reactions with isopentenyl pyrophosphate, a highly flexible loop 72−83 was previously linked to protein conformational change required for catalysis [Chen, Y. H., Chen, A. P.-C., Chen, C. T., Wang, A. H.-J., and Liang, P. H., (2002) *J. Biol. Chem. 277*, 7369−7376]. The crystal structure and fluorescence studies suggested that the α3 helix connected to the loop moves toward the active site when the substrate is bound. To identify the active conformation and study the role of the loop for conformational change, the UPPs mutants with amino acids inserted into or deleted from the loop were examined. The inserted mutant with extra Ala residues fails to display the intrinsic fluorescence quenching upon FPP binding, and its crystal structure reveals only the open form. These phenomena appear to be different from the wild-type enzyme in which open and closed conformers were observed and suggest that the extended loop fails to pull the α3 helix and/or the extra amino acids in the loop cause steric hindrance on the α3 helix movement. The loop-shortening mutants with deletion of V82 and S83 or S72 also adopt an open conformation with the loop stretched, although they show decreased intrinsic fluorescence with FPP bound, similar to that seen in the wild-type enzyme. We conclude that the closed conformation is apparently the active conformation. Change of the length of the loop 72−83 impairs the ability of conformational change and causes remarkably lower activity of UPPs.

Undecaprenyl pyrophosphate synthase (UPPs)[1] is a *cis*-prenyltransferase, which catalyzes eight consecutive condensation reactions of C_5-isopentenyl pyrophosphate (IPP) with C_{15}-farnesyl pyrophosphate (FPP) to generate C_{55}-undecaprenyl pyrophosphate (UPP) with newly formed double bonds in cis configuration (*1*−*3*). UPP acts as a lipid carrier to mediate the synthesis of bacterial cell wall peptidoglycans (*4*, *5*). The crystal structures of UPPs from *Micrococcus luteus* and *Escherichia coli* have recently been solved (*6*, *7*). We proposed that a tunnel-shaped crevice surrounded by two α helices (α2 and α3) and four β strands (βA, βB, βD, and βC) with hydrophobic residues lined in its interior surface is the active site of *E. coli* UPPs (*7*). The tunnel provides the space for FPP binding on the top to undergo chain elongation by condensation with IPP, and the bottom of the tunnel is sealed by L137 (*7*, *8*). Each newly formed intermediate is moved downward in the tunnel, thereby allowing the entrance of IPP for the next cycle of condensation reaction. Finally, a large product needs to exit from the active site, which represents the rate-limiting step (*9*, *10*). Apparently, the protein structure possesses a great deal of flexibility for its catalysis.

Conformational change was found essential for UPPs catalysis (*11*). Two protein conformers, namely, closed and open forms,[2] were observed for the two subunits in the crystal structure of *E. coli* UPPs, which differ in the location of the kink in α3 (*7*). According to the 3-D structure, the enzyme adopts a closed conformation when a single Triton (substrate-like) is bound (*7*). In contrast, the open form either contains only water or has two Triton molecules bound (product-like) in the active site (*12*). Triton at low concentration (0.1%) stimulated the enzyme activity by facilitating the product release (*9*), but high concentration of Triton (>1%) inhibited the enzyme activity by occupying the active site (*12*). The interchange between the open and the closed forms was speculated to participate in the substrate binding and product

† This work was supported by grants from Academia Sinica to A.H.-J.W. and P.H.L.

* To whom correspondence should be addressed. (P.H.L): e-mail: phliang@gate.sinica.edu.tw. Tel: +886−2−2785−5696 ext. 6070. Fax: +886−2−2788−9759; (A.H.-J.W.): e-mail: ahjwang@gate.sinica.edu.tw. Tel: +886−2−2788−1981. Fax: +886−2−2788−2043.

[1] Abbreviations: UPPs, undecaprenyl pyrophosphate synthase; UPP, undecaprenyl pyrophosphate; IPP, isopentenyl pyrophosphate; FPP, farnesyl pyrophosphate; DDPPs, dolichyl pyrophosphate synthases; FPPs, farnesyl pyrophosphate synthase; DPPs, decaprenyl pyrophosphate synthase; PPPs, polyprenyl pyrophosphate synthase; Hepes, 4-(2-hydroxyethyl)-1-piperazineethanesulfonic acid; SDS−PAGE, sodium dodecyl sulfate−polyacrylamide gel electrophoresis.

[2] Throughout this paper, the open and closed forms are defined on the basis of the local structure in the α3 helix of UPPs. In the open form, the upper portion of the α3 helix is straight, whereas in the closed form, it is kinked and bent toward the α2 helix (see Figure 5).

10.1021/bi035283x CCC: $25.00
Published on Web 11/15/2003

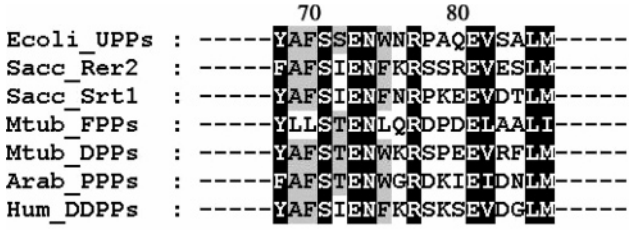

FIGURE 1: Alignment of amino acid sequences in the region of the conserved loop of the *E. coli* UPPs, yeast DDPPs Rer2 and Srt1, *M. tuberculosis* FPPs Rv1086, *M. tuberculosis* DPPs Rv2361c, *Arabidopsis thaliana* PPPS, and human DDPPs. Black and gray outlines indicate identical and similar amino acid residues, respectively. The length of the loop is conserved in these enzymes. As shown in Figure 5, the totally conserved amino acids including S71, E73, N74, R77, and E81 are facing the active site and likely play roles for substarte binding and atalysis.

release (*7*, *11*, *12*). Upon FPP binding, the intrinsic fluorescence intensity of W91 is decreased, suggesting different environments of W91 between the free and substrate-bound forms (*11*). W91 is located in the α3 helix that moves toward the substrate site upon FPP binding to form a closed conformation to facilitate the reaction (*7*). After the reaction is completed and the product reaches the desired chain length, the UPPs will reopen to release the product. The increase and decrease in intrinsic fluorescence using stop-flow experiments suggest the conformational change during catalysis (*11*). However, it was not clear regarding the control mechanism of the conformational change.

A flexible loop (amino acids 72−83) in *E. coli* UPPs connecting α3 and *β*B may play a key role in mediating the conformational change associated with the α3 helix. This loop is invisible in the previous crystal structure of the UPPs probably due to its high disorder required for its function (*7*). The length of this flexible loop appears critical in *cis*-prenyltransferases including *E. coli* UPPs, yeast, and human dolichyl pyrophosphate synthases (DDPPs), *M. tuberculosis* farnesyl pyrophosphate synthase (FPPs), and decaprenyl pyrophosphate synthase (DPPs), as well as an *Arabidopsis thaliana* polyprenyl pyrophosphate synthase (PPPs) based on sequence alignment (Figure 1) (*3*). Their loop regions have the same number of amino acids and several residues are conserved. However, only the crystal structure of UPPs among *cis*-prenyltransferases is known, and this serves as a model to understand the catalysis of others in the family. Kinetic measurements of *E. coli* UPPs mutants with several of the conserved amino acids in the loop replaced by Ala indicated the importance of the loop for the substrate binding and catalysis (*7*). Substitution of S71 or E81 in the loop with Ala greatly increased IPP K_m value and W75A mutation increased both FPP and IPP K_m values (*7*, *13*). Furthermore, S71A, E73A, N74A, R77A, and E81A all show significantly reduced k_{cat} values (*7*).

From these previous studies, it remains unclear regarding the role of this loop associated with the protein conformational change. The loop could just passively provide the support as α3 moves during the conformational change upon substrate binding. Alternatively, the loop could act like a spring and provides the driving force to trigger the conformational relocation of α3. Our crystal structure of UPPs in complex with FPP substrate (unpublished results) shows that residues 72, 82, and 83 are distant from the bound FPP (>10 Å). Moreover, S72 and S83 are not conserved in the aligned amino acid sequences in the loop region (aa 72−83) of UPPs and its homologues (see Figure 1). These results led us to believe that those three amino acids 72, 82, and 83 are most suitable to delete or insert amino acids to examine the importance of the loop length associated with conformational change in UPPs. On the other hand, the strictly conserved S71, E73, N74, R77, and E81 in the middle of the loop play an important function in catalysis and are not suitable for deletion. In the present study, we have inserted or deleted amino acids in the regions of amino acids 72 and 83 and characterized these mutants by fluorescence binding assay, kinetic parameter determination, and 3-D structural studies.

EXPERIMENTAL PROCEDURES

Reagents and General Methods. Radiolabeled [^{14}C]IPP (55 mCi/mmol) was purchased from Amersham Pharmacia Biotech, and FPP was obtained from Sigma. Reversed-phase thin-layer chromatography (TLC) plates were purchased from Merck. *Taq* DNA polymerase was obtained from TaKaRa. The plasmid mini-prep kit, DNA gel extraction kit, and NiNTA resin were purchased from Qiagen. Potato acid phosphatase (2 units/mg) was purchased from Roche Molecular Biochemicals. FXa and the protein expression kit (including the pET32Xa/LIC vector and competent JM109 and BL21 cells) were obtained from Novagen. All commercial buffers and reagents were of the highest grade.

Preparation of Insertion and Deletion Mutant UPPs. UPPs mutants were prepared by using PCR techniques with the template of *E. coli Bos-12* UPPs gene cloned in the pET32Xa/Lic vector. The mutagenic primers used were prepared by MDBio Inc. (Taiwan). The mutagenic oligonucleotides for performing site-directed mutagenesis are as follows: forward primer 5′-GCGGCAGCCGCAGCTGCGTTAATGGAACTG-3′ and reverse primer 5′-AGCTGCGGCTGCCGCACTGACTTCCTGCGC-3′ for $S^{83}(Ala)_5$; forward primer 5′-CAGGAAGTCAGTGCGGCGTTAATGGAACTG-3′ and reverse primer 5′-TTCCATTAACGCCGCACTGACTTCCTGCGC-3′ for $S^{83}(Ala)_1$; forward primer 5′-AGTCGCGTTAATGGAACTGTT-3′ and reverse primer 5′-ACGCGACTTCCTGCGCTGGTC-3′ for ΔS83; forward primer 5′-GGAAGCGTTAATGGAACTGTTTG-3′ and reverse primer 5′-ACGCTTCCTGCGCTGGTCGGTTC-3′ for ΔV82S83 double deletion mutant. For construction of ΔS72, two forward primers 5′-AGTGAAAACTGGAACCG-3′ and 5′-CTTTAGTGAAAACTGGAACCG-3′ and two reverse primers 5′-AAAGGCATACAGCGTTA-3′ and 5′-CACTAAAGGCATACAGCGTTA-3′ were used. Subsequently, the forward primer 5′-GGTATTGAGGGTCGCATGTTGTCTGCT-3′ and reverse primer 5′-AGAGGAGAGTTAGAGCCATCAGGCTGT-3′ were used in combination with the PCR products obtained using the above mutagenic oligonucleotides to create the full-length mutant UPPs genes. The FXa cleavage site (IEGR) and the complementary sequences to the sticky ends of the linear vector pET-32Xa/LIC were included in these primers. Thirty cycles of PCR were performed using a thermocycler (Applied Biosystems) with the melting temperature at 95 °C for 2 min, annealing temperature at 45 °C for $S^{83}(Ala)_5$ and 52 °C for other mutants for 1 min, followed by polymerization temperature at 68 °C for 1 min. Expression and purification of the mutant proteins were carried out as previously described (*8*).

Measurements of K_m and k_{cat} Values for Mutant UPPs. For the measurements of kinetic parameters, mutant UPPs (1 μM $S^{83}(Ala)_5$, $S^{83}(Ala)_1$, ΔV82S83, ΔS83 or 2 μM ΔS72) was utilized to initiate the reaction of FPP with [^{14}C]IPP in 200-μL solution. For IPP K_m and k_{cat} determinations, 10 μM FPP was utilized to saturate the enzyme, and IPP concentrations of 0.2−400 μM were employed. For FPP K_m measurements, 0.2−25 μM FPP were used along with 20 μM [^{14}C]IPP. All reactions were carried out in 100 μM KOH−Hepes buffer, pH 7.5, 50 mM KCl, and 0.5 mM $MgCl_2$ at 25 °C in the presence of 0.1% Triton X-100. To measure the initial rate, 40-μL portions of the reaction mixture were periodically withdrawn within 10% substrate depletion and mixed with 10 mM EDTA for reaction termination. The radiolabeled products were then extracted with 1-butanol, and the radioactivities associated with aqueous and butanol phases were separately quantitated by using a Beckman LS6500 scintillation counter. Initial velocity data were fitted to Michaelis−Menten equation to obtain K_m and k_{cat} values by nonlinear regression using the KaleidaGraph computer program (*14*). For product identification, the butanol extracted radiolabeled products were converted to alcohols by potato acidic phosphatase and separated on reverse-phase TLC as described previously (*15*).

Fluorescence Binding Experiments. The changes of mutant UPPs intrinsic fluorescence upon the addition of FPP were monitored using a F-4500 fluorescence spectrophotometer (Hitachi, Japan). The emission spectra were recorded from 300 to 450 nm upon excitation of wild-type and mutant UPPs at 285 nm. The fluorescence spectra of 1 μM enzyme in a buffer containing 100 mM KOH−Hepes (pH 7.5), 0.5 mM $MgCl_2$, and 50 mM KCl at 25 °C were measured before and after the addition of 15 μM FPP to observe the protein conformational change.

Crystallographic Analysis. The purified UPPs mutants were crystallized using the hanging drop setup from Hampton Research (Laguna Niguel, CA). In the end, 2 μL of mother liquid containing 25% PEG400 for $S^{83}(Ala)_5$, ΔS72 and 15% PEG400 for ΔV82S83 in 100 mM sodium cacodylate at pH 5.5 were mixed with 2 μL of protein solution of 10 mg/mL mutant UPPs, 1% Triton X-100, 3 mM $MgCl_2$. The mixture was equilibrated against 200 μL of the mother liquid at 25 °C. Isomorphous crystals started to appear within 2 days. Diffraction experiments of the mutant UPPs crystals were carried out at −150 °C on beam line 17B2 of the National Synchrotron Radiation Research Center in Hsinchu, Taiwan. Data were processed and scaled by employing the program HKL2000 (*16*). For computational refinement, manual modification, and analysis of the crystal structure, the programs CNS, O, and CCP4 were used (*17*−*19*).

RESULTS

Generation of Loop Insertion and Deletion Mutants of UPPs. By using PCR with the primers listed in the Experimental Procedures, the genes of mutant *E. coli* UPPs including $S^{83}(Ala)_5$ and $S^{83}(Ala)_1$ with insertion of one and five extra Ala and the mutants with deletion of S83, S72, or both V82 and S83 were constructed and expressed using *E. coli* BL21 as host cells under the control of T7 promoter. It is critical that different codons were used for Ala in preparing the mutants to prevent the annealing of mutagenic PCR products at wrong positions so that correct number of Ala residues can be inserted. For preparing the deletion mutant ΔS72, a second pair of mutagenic forward and reverse primers was utilized to increase the overlapping of nucleotides. The purification of the His-tagged proteins was achieved using NiNTA column chromatography. The tag was removed by using FXa protease and the untagged UPPs was recovered by a second NiNTA. This procedure gave highly pure mutant enzymes as judged by SDS−PAGE (Figure 2A).

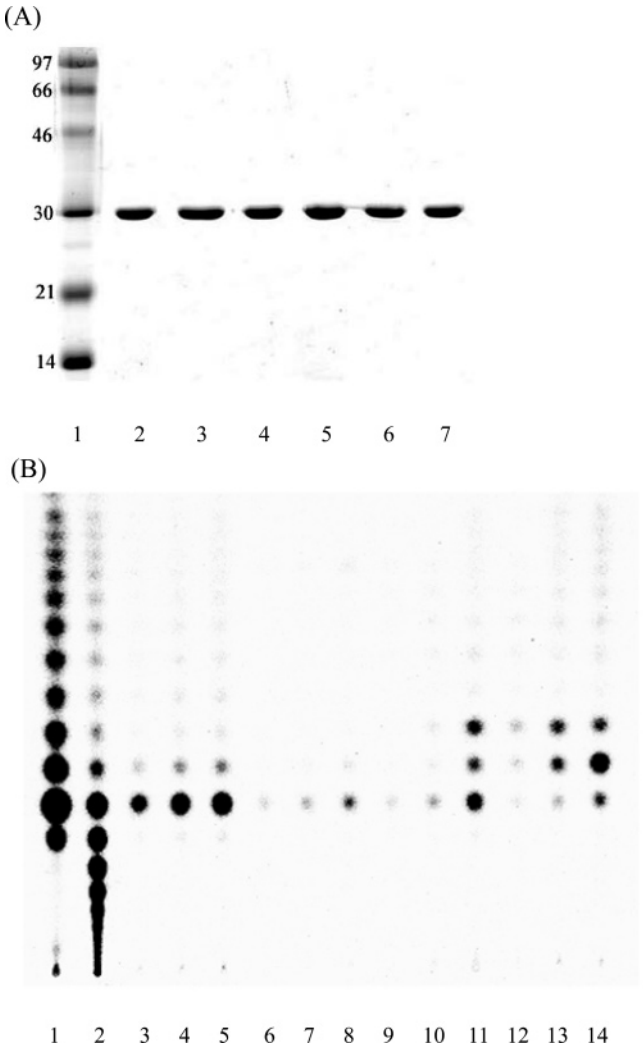

FIGURE 2: SDS−PAGE analysis of the mutant UPPs generated in this study (A). The lanes from left to right contain the molecular weight standards (lane 1), wild-type UPPs (lane 2), $S^{83}(Ala)_5$ (lane 3), $S^{83}(Ala)_1$ (lane 4), ΔS72 (lane 5), ΔS83 (lane 6), and ΔV82S83 (lane 7). The products generated by the loop insertion and deletion mutants (B). Lanes 1 and 2 represent the products of wild-type UPPs generated in the presence and absence of 0.1% Triton X-100 as shown in our previous paper (*8*). With Triton, the intermediates plus the C_{55} product were produced, whereas in the absence of Triton, the C_{55} and longer products were generated. These serve as markers for identification of products generated by UPPs mutants. As shown in lanes 3−5, 6−8, 9−11, and 12−14 are the products generated after reaction for 1, 3, and 9 h for mutants $S^{83}(Ala)_5$, ΔS72, ΔS83, ΔV82S83, respectively. The final products for these mutants were C_{55} except that ΔV82S83 mainly produced C_{50} product in the time range.

Kinetic Parameter Determination of the Mutant UPPs. As shown in Table 1, all mutants with elongated or shortened loop showed remarkably (10^4−10^5-fold) lower activities than

Table 1: Kinetic Parameters of the Wild-Type and Mutant UPPs Including $S^{83}(Ala)_5$, $S^{83}(Ala)_1$, ΔV82S83, ΔS83, and ΔS72

UPPs	k_{cat} (s^{-1})	FPP K_m (μM)	IPP K_m (μM)
wild type	2.5	0.4 ± 0.1	4.1 ± 0.3
$S^{83}(Ala)_5$	1.3×10^{-4}	0.17 ± 0.03	7.8 ± 1.3
$S^{83}(Ala)_1$	9.0×10^{-4}	0.4 ± 0.2	34 ± 5
ΔV82S83	2.2×10^{-4}	1.8 ± 0.2	>3000
ΔS83	7.6×10^{-5}	1.0 ± 0.2	>3000
ΔS72	2.8×10^{-5}	0.5 ± 0.1	11.7 ± 2.6

the wild-type UPPs, indicating *the strict stringency on the length of the loop in enzyme catalysis*. Even with one Ala insertion, the k_{cat} of $S^{83}(Ala)_1$ is 10^4-fold smaller (see Table 1). Insertion of five Ala in $S^{83}(Ala)_5$ did not significantly change the FPP and IPP K_m values compared to the wild type, suggesting its similar affinity with the substrates. However, as shown below from the crystal structure, the extension of the loop freezes the mutant UPPs in the open conformer. This mutant has extremely poor activity due to its incapability of undergoing protein conformational change. The deletion of S72, S83, or V82/S83 did not lead to a significant change of the FPP K_m value either. However, both ΔS83 and ΔV82S83 have remarkably larger IPP K_m values compared to the wild-type UPPs. Interestingly, despite the altered K_m and k_{cat} values, most of the mutants generated C_{55} except that ΔV82S83 produced mainly C_{50}, one IPP unit shorter in the specified reaction time (Figure 2B).

Fluorescence Binding Experiments. According to our previous studies, the FPP binding quenches the W91 fluorescence, and this serves as an indicator for protein conformational change from the open to the closed form (*11*). As shown in Figure 3A, the wild-type UPPs intrinsic fluorescence is decreased by the binding of FPP as previously shown. In contrast to the wild type, the mutant $S^{83}(Ala)_5$ displayed no significant change of fluorescence upon substrate binding (see Figure 3B). This is consistent with the finding that insertion of five extra Ala residues into the loop has locked the 3-D structure of mutant UPPs in the open form as shown below even with a Triton bound in the active site. However, the wild-type enzyme shows only the closed form when a Triton is bound in the active site (one single molecule of Triton mimics the substrate) (*12*). The $S^{83}(Ala)_1$ with one extra Ala also failed to show intrinsic fluorescence change with addition of FPP (data not shown). In contrast, Δ83, ΔV82S83, and Δ72 have shown altered fluorescence upon FPP binding with similar amplitude to that of the wild type (Figure 3C). Surprisingly, these mutants still adopt an open structure with Triton bound in the active site as shown below.

3-D Structure of $S^{83}(Ala)_5$ and ΔV82S83 Mutants. The difference Fourier maps of $S^{83}(Ala)_5$, ΔV82S83, and ΔS72 were phased by using the refined structure of wild-type UPPs (*11*). The parameters for ideal protein geometry from Engh & Huber (*20*) were used for the refinements, and the stereochemical quality of the refined structures was checked with the program PROCHECK (*21*). Both R-factor and R_{free} were used to monitor the progress of structural refinement. The data collection and refinement statistics are summarized in Table S1 (Supporting Information). The refined model of $S^{83}(Ala)_5$ in complex with Triton contains amino acid residues 13−70, 83−239 in one subunit (monomer A) and 15−70, 86−238 in the other subunit (monomer B). Figure

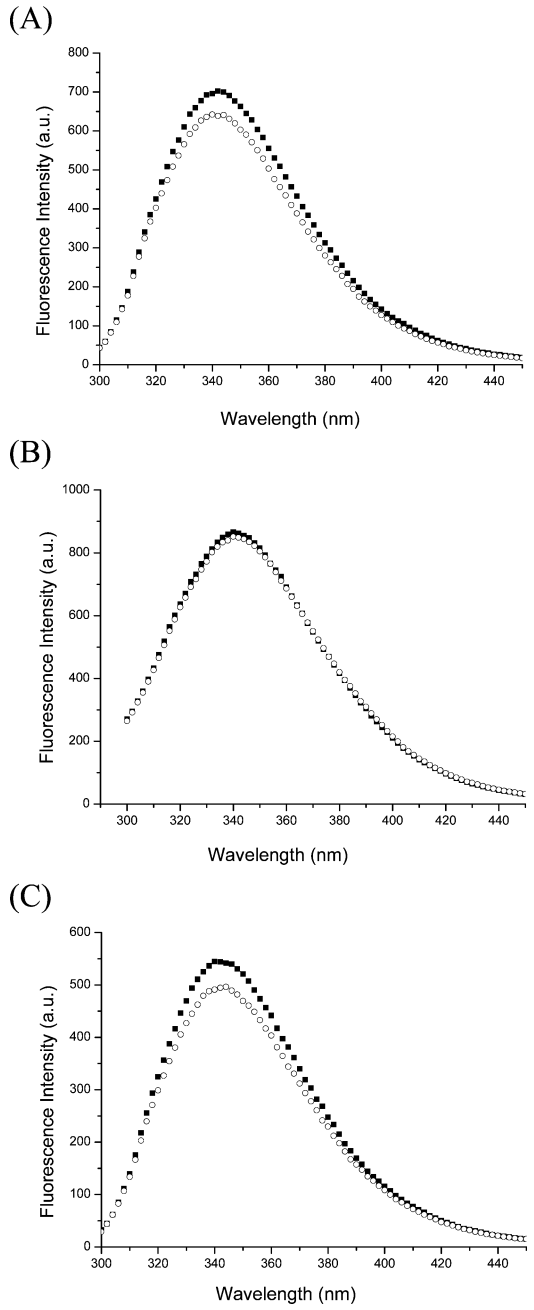

FIGURE 3: Change of 1 μM mutant UPPs fluorescence by addition of 15 μM FPP. The fluorescence intensity of the protein (■) and that (○) of protein in complex with FPP are shown. The wild-type fluorescence is decreased by addition of FPP (A). For the insertion mutant $S^{83}(Ala)_5$, the change of protein fluorescence is negligible (B). FPP binding quenches the fluorescence of ΔS72 in similar amount compared to the wild type (C). The fluorescence emission spectra of the samples from 300 to 450 nm were recorded at pH 7.5 and 25 °C in the buffer.

4A,B shows ribbon diagrams of the dimeric $S^{83}(Ala)_5$ structure for monomer A and B, respectively. In our previous studies, we found that two Triton molecules mimicking the product in the active site render UPPs to adopt an open conformation (*12*), whereas a substrate-like single Triton makes the enzyme to adopt a closed conformation (*7*). In the $S^{83}(Ala)_5$ structure, one Triton X-100 molecule is bound to the top portion of the active site tunnel of monomer A, and another Triton X-100 molecule on the bottom of monomer B active site (Figure 4A,B). The two subunits

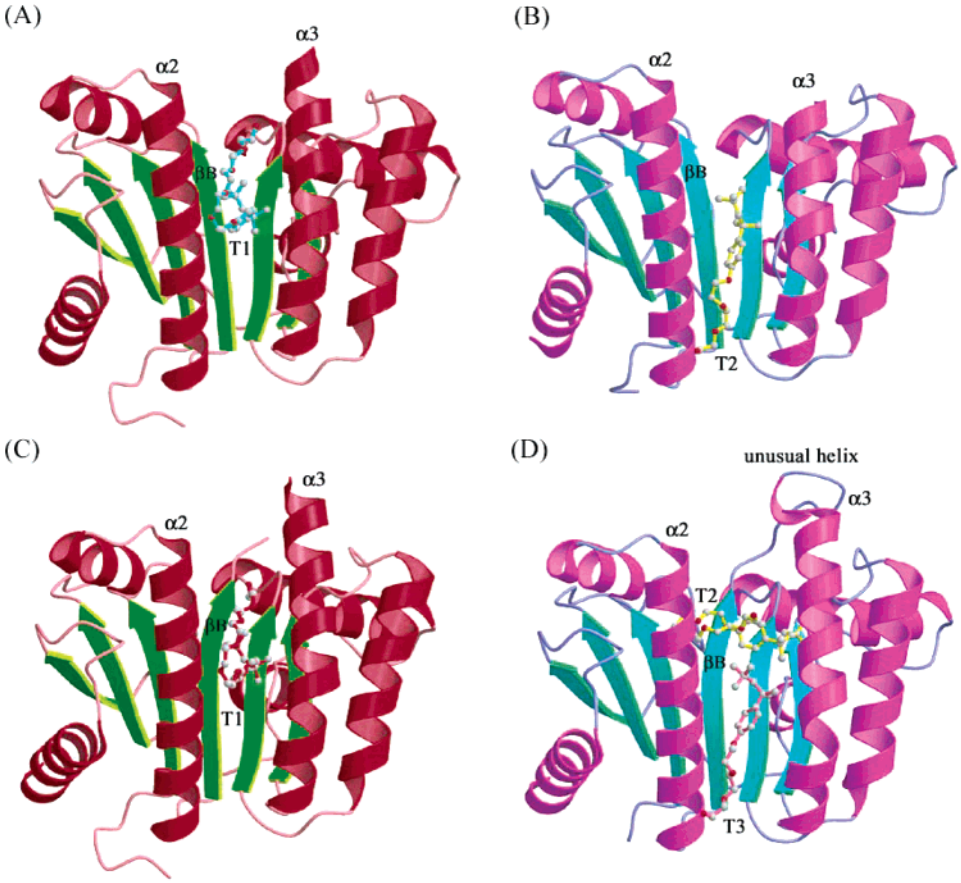

FIGURE 4: The crystal structure of $S^{83}(Ala)_5$ for subunit A and B shown in (A) and (B), respectively. One Triton X-100 (T1) molecule is bound to the top portion of the active site tunnel of monomer A, and the other Triton X-100 (T2) molecule on the bottom of monomer B active site. The two subunits have similar structures as the open form observed in the apo-enzyme crystal except that a stretch of amino acids in helices α3 is invisible suggesting the more disordered structure resulted from the extension of the loop. In (C) and (D) are the 3-D structure of ΔV82S83 for monomer A and B, respectively. Three Triton (T1, T2, and T3) are located in the two monomers with one on the top portion of the active site tunnel in monomer A and the other two occupying the overall tunnel of monomer B. The Fourier map for the loop residues 70−78 in monomer B is clearly visible in contrast to previous results. The shortened loop utilizes 76−78 to replace amino acids 82−83 for maintaining an unusual helix form but the whole loop is stretched with reduced flexibility.

showed similar structures to that of the open form observed in the apo-enzyme crystal, except that a stretch of amino acids in α3 helix is invisible probably due to high mobility in that region. It is notable that *β*B in the insertion mutant adopts the same position (pointed to the left) as the closed form of the wild-type UPPs due to the elongated loop that gives flexibility of *β*B (see Discussion below).

As shown in Figure 4C,D, three Triton molecules are located in the two monomers of the ΔV82S83 structure: one on the top portion of the active site tunnel in monomer A, and the other two occupy the entire tunnel of monomer B. The refined model of ΔV82S83 contains amino acid residues 13−72, 79−239 in monomer A, and 15−239 in monomer B. The Fourier map for the loop residues 70−78 in monomer B is clearly visible. The shortened loop utilizes 76−78 to replace amino acids 82−83 for maintaining an unusual helix form, but the entire loop is stretched and has reduced flexibility. In both subunits A and B, open conformations were observed.

Compared to $S^{83}(Ala)_5$, the structure of ΔV82S83 shows displacements of residues 69−70 at the C-terminus of strand *β*B. This displacement is probably due to the reduced length of the loop which may cause strand *β*B being dragged toward α3. Preceding the α3 helix, an unusual helix is formed (Figure 4D). The loop region in the deletion mutant is more apparent due to its constrained motion of the loop. The structure of mutant ΔS72 with a single amino acid deleted displays similar feature of structure (data not shown).

Our results described above show that the open forms in both insertion and deletion mutants have 10^4-fold lower activities than that of wild-type UPPs. The wild type has been shown to adopt the closed conformation when a substrate-like single Triton is bound and the open conformation when the product-like two Triton molecules are in the active site. It is obvious from our present study that the closed conformation is the active form during UPPs catalysis, whereas the open form is relatively inactive. In Figure 5A,B, the closed form from the apo-UPPs A-chain (*7*) and the open conformation from two Triton-bound UPPs B-chain (*12*) are superimposed. The hydrophobic amino acids including L85, F89, L88, and L93 in the upper portion of the α3 helix are faced toward the active site in the closed form, whereas L88′, F89′, and W91′ in the open form are more outward. As shown in panel 5B, the F70 and S71 are near the S1 and S2 substrate site in the closed form, whereas in the open form they are in distal positions. The importance of F70 and S71 in UPPs catalysis had been demonstrated in previous site-directed mutagenesis studies (*13*). These dispositions of

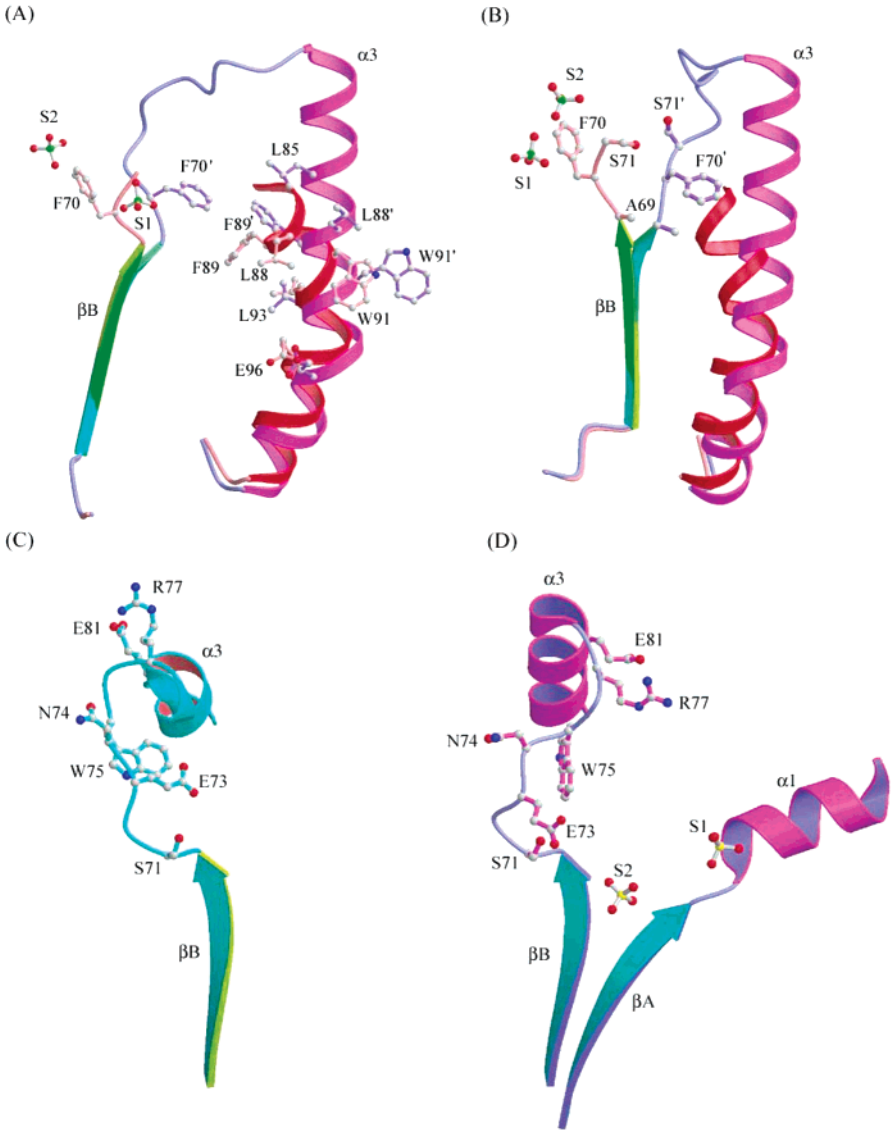

FIGURE 5: (A) and (B) are two representations of superimposed structures of the open and closed forms of wild-type UPPs. The closed conformation from apo-UPPs A-chain (*7*) is shown in green and red, and the open conformation from two Triton-bound UPPs B-chain (*12*) is shown in cyan and purple for the βB strand and α3 helix, respectively. Two sulfate ions (S1 and S2) represent the sites of substrates. In the left model, side chains of L85, L88, F89, and W91 in the closed form are kinked toward the active site and show significant dispositions as indicated by L85′, L88′, F89′, and W91′ in the open form. All these hydrophobic residues lined in the interior surface of α3 helix stabilize the extended carbon chains as condensation reactions occur. In the right model focusing on positions of amino acids just before the loop, the F70 and S71 of the closed-form are closer to substrate site in contrast to the F70′ and S71′ of the open-form. The above results explain that the closed form is active but open form is inactive as proposed in the present study. (C) and (D) show the comparison of the positions of important amino acids in the loop regions of ΔV82S83 and wild-type UPPs, both in open forms. In (C), ΔV82S83 encompasses a connection between the βB strand and the α3 helix, shown in light green, and the wild type in (D) is shown with the strand and helix colored in green and purple. For wild type, E81, R77, W75, and E73 are oriented toward the substrate binding locations (S1 and S2), so when it forms closed form, these residues assist substrate binding and catalysis. In contrast, these amino acids in ΔV82S83 are oriented away from the active sites. These amino acids in the loop have been shown to be the key residues for catalysis from our previous site-directed mutagenesis study (*7*).

active site amino acids guarantee better catalytic efficiency in the closed form.

Several amino acids S71, E73, N74, W75, R77, and E81 in the loop were found important to UPPs substrate binding and reaction (*7*). The present X-ray structure of the loop mutants lends support for these observations. In the loop-shortening mutant ΔV82S83 that adopts the open conformation, these residues are away from the active site (Figure 5C). In contrast, the wild-type UPPs in the open conformation has E81, R77, W75, E73, and S71 facing to the substrate site (S1 and S2) (Figure 5D). When the wild-type UPPs undergoes a conformational change from the open to the closed form, the correct amino acids in the loop can clamp down to bind the substrates and initiate the reaction. It appears that the closed form is active and the reaction occurs with much higher efficiency compared to the open form.

DISCUSSION

Since the early study on the binding plasticity of serum albumin pointing out the importance of structural ensembles for function (*22*), intrinsic disorder has been mostly ignored until recently (*23*, *24*). Many proteins have been shown by limited proteolysis, CD, NMR, X-ray, and other methods to display disordered structures that are essential for their

functions (*24*). In the crystal structure of UPPs, a flexible loop composed of amino acid 72−83 was found to be critical for substrate binding and enzyme catalysis (*7*). Addition of FPP substrate induces the movement of α3 from an open to a closed conformation, and the large final product switches the closed form to the open form for release (*7*, *12*). In the present study, we have reported the essential role of the loop 72−83 in triggering such a conformational change by constructing the insertion and deletion mutants and examining their kinetic parameters, conformational change using fluorimeter as well as the 3-D structures.

On the basis of the present crystal structure, the extended loop mutant $S^{83}(Ala)_5$ has locked the protein conformation in the open form. The extra Ala residues largely increased the flexibility of the loop as evidenced from the invisible electron density in the X-ray structure (Figure 4A,B). The highly flexible loop with extended length fails to pull the α3 to induce a conformational change. Alternatively, these redundant amino acids in the loop may cause steric hindrance to prevent the movement of α3 toward α2. The intrinsic fluorescence decrease as seen in the binding of FPP to the wild-type protein was not found in $S^{83}(Ala)_5$. This mutant enzyme shows a 10^4-fold smaller k_{cat} value but still binds substrates with similar K_m values compared to the wild type. Apparently, the α3 movements are essential for optimal catalysis but not for the FPP binding. We also observed that with only one Ala inserted into the loop after the end (S83) of the loop it still significantly impaired the enzyme activity.

On the other hand, the loop deletion mutants should have higher activity since the reduction of loop length may force α3 to adopt the closed conformation which is more active. Surprisingly, the observed crystal structure shows an open form in both subunits, similar to the structure of the insertion mutant, but the loop is stretched due to its smaller length (Figure 4C,D). Different from the open form of the wild type and insertion mutants, *β*B of ΔV82S83 is pulled to the right toward α3 and α3 retains in the open conformation. Although the addition of FPP indeed quenches the fluorescence of the deletion mutant, indicating that a metastable closed conformation may occur during enzyme turnover, the smaller length of the loop must interfere with the conformational change as suggested by its extremely low k_{cat} and open-form crystal structure with Triton bound. However, the deletion or insertion of residues may not only change the position of large secondary structures but also undoubtedly reorient residues in the loop. Such a reorientation may move key residues required for catalysis out of a most favored position and cause lower enzyme activity.

In the wild-type UPPs, the fluorescence of W91 located in α3 is quenched by FPP binding (*11*). From the crystal structure, the α3 is distant from the active site in the absence of substrate. It is the loop which connects α3 and brings this helix close to α2 and creates a pocket for the substrate binding. Upon product formation, *β*B is reoriented from left to right, seemingly induced through the loop, while α3 switches from the closed to the open conformation. When the loop is extended by incorporating five extra Ala, α3 maintains in the open position but *β*B is directed to the left with a substrate-like Triton bound in the active site (Figure 4A,B). On the other hand, the loop shortening results in open conformation with *β*B directed to right with Triton bound (Figure 4C,D). The k_{cat} of the insertion and deletion mutants are extremely low indicating that the open form is relatively inactive with 10^4-fold lower specific activity whereas the closed form is active. As illustrated in Figure 5, the closed form has several amino acids in α3 helix and the loop, which likely participate in substrate binding and catalysis, at the favorable positions for reaction. The conformational change from inactive to active form is thus required for enzyme catalysis. With the insertion or deletion of amino acids, the mutation impairs the conformational change leading to lower activities. Only with the correct length and the conserved amino acids in the loop, the *E. coli* UPPs can undergo conformational change to the active closed form for reaction and conversion to open form after reaction for product release.

ACKNOWLEDGMENT

Authors thank the useful suggestion from Dr. A. K. Dunker. We are grateful to Dr. Tzu-Ping Ko and Mr. Kai-Fa Huang for technical assistance. We also thank National Synchrotron Light Source for the use of synchrotron data collection.

SUPPORTING INFORMATION AVAILABLE

Data collection and refinement statistics of $S^{83}(Ala)_5$, ΔV82S83, and ΔS7 (Table S1). This material is available free of charge via the Internet at http://pubs.acs.org.

REFERENCES

1. Allen, C. M. (1985) *Methods Enzymol. 110*, 281−299.
2. Ogura, K., and Koyama, T. (1998) *Chem. Rev. 98*, 1263−1276.
3. Liang, P. H., Ko, T. P., and Wang, A. H.-J. (2002) *Eur. J. Biochem. 269*, 3339−3354.
4. Ogura, K., Koyama, T., and Sagami, H. (1997) *Sub-cellular Biochemistry*, Vol. 28, Chapter 3, pp 57−87, Plenum Press, NY.
5. Robyt, J. (1998) in *Essentials of Carbohydrate Chemistry*, Chapter 10, pp 305−318, Springer-Verlag, New York.
6. Fujihashi, M., Zhang, Y.-W., Higuchi, U., Li, X.-Y., Koyama, T., and Miki, K. (2001) *Proc. Natl. Acad. Sci. U.S.A. 98*, 4337−4342.
7. Ko, T. P., Chen, Y. K., Robinson, H., Tsai, P. C., Gao, Y.-G., Chen, A. P.-C., Wang, A. H.-J., and Liang, P. H. (2001) *J. Biol. Chem., 276*, 47474−47482.
8. Pan, J. J., Yang, L. W., and Liang, P. H. (2000) *Biochemistry 39*, 13856−13861.
9. Pan, J. J., Chiou, S. T., and Liang, P. H. (2000) *Biochemistry 39*, 10936−10942.
10. Chen, A. P.-C., Chen, Y. H., Liu, H. P., Li, Y. C., Chen, C. T., and Liang, P. H. (2002) *J. Am. Chem. Soc. 124*, 15217−15224.
11. Chen, Y. H., Chen, A. P.-C., Chen, C. T., Wang, A. H.-J., and Liang, P. H. (2002) *J. Biol. Chem. 277*, 7369−7376.
12. Chang, S. Y., Ko, T. P., Liang, P. H., and Wang, A. H.-J. (2003) *J. Biol. Chem. 278*, 29298−29307.
13. Fujikura, K., Zhang, Y.-W., Yoshizaki, H., Nishino, T., and Koyama, T. (2000) *J. Biochem. 128*, 917−922.
14. Segel, I. H. (1993) in *Enzyme Kinetics: Behavior and Analysis of Rapid Equilibrium and Steady-State Enzyme Systems*, pp 100−118, John Wiley and Sons, New York.
15. Fujii, H., Koyama, T., and Ogura, K. (1983) *Biochim. Biophys. Acta 712*, 716−718.
16. Otwinowski, Z., and Minor, W. (1997) *Methods Enzymol. 276*, 307−326.
17. Brunger, A. T., et al. (1998) *Acta Crystallogr. Sect. D 54*, 905−921.
18. Jones, T. A., Zou, J. Y., Cowan, S. W., and Kjeldgaard, M. (1991) *Acta Crystallogr. Sect. A 47*, 392−400.

19. Collaborative Computational Project Number 4. (1994) *Acta Crystallogr. Sect. D 50*, 760−763.
20. Engh, R. A., and Huber, R. (1991) *Acta Crystallogr. A 47*, 392−400.
21. Laskowski, R. A., MacArthur, M. W., Moss, D. S., and Thornton, J. M. (1993) *J. Appl. Crystallogr. 26*, 283−291.
22. Karush, F. (1950) *J. Am. Chem. Soc. 72*, 2705−2713.
23. Dyson, H. J., and Wright, P. E. (2002) *Curr. Opin. Struct. Biol. 12*, 54−60.
24. Dunker, A. K., Brown, C. J., Lawson, D., Iakoucheva, L. M., and Obradovic Z. (2002) *Biochemistry 41*, 6573−6582.

BI035283X